frontiers in Applied Mathematics and Statistics

TYPE Original Research
PUBLISHED 30 October 2026
DOI 10.3389/fams.2026.1981280

Check for updates

OPEN ACCESS

EDITED BY
Haitao Song,
Shanxi University, China

REVIEWED BY
Fahad Al Basir,
Asansol Girls' College, India
Mideksa Tola Jiru,
Arsi University, Ethiopia

*CORRESPONDENCE
Ebenezer Kwesi Lotey
ebenezerlotey92@gmail.com

RECEIVED 28 August 2026
REVISED 02 October 2026
ACCEPTED 16 October 2026
PUBLISHED 30 October 2026

CITATION
Boateng FO and Lotey EK (2026) Modeling the spread and mitigation of absenteeism among university students: a stage-structured compartmental approach with optimal control. *Front. Appl. Math. Stat.* 12:1981280. doi: 10.3389/fams.2026.1981280

COPYRIGHT
© 2026 Boateng and Lotey. This is an open-access article distributed under the terms of the Creative Commons Attribution License (CC BY). The use, distribution or reproduction in other forums is permitted, provided the original author(s) and the copyright owner(s) are credited and that the original publication in this journal is cited, in accordance with accepted academic practice. No use, distribution or reproduction is permitted which does not comply with these terms.

Modeling the spread and mitigation of absenteeism among university students: a stage-structured compartmental approach with optimal control

Francis Ohene Boateng and Ebenezer Kwesi Lotey*

Department of Mathematics Education, Akenten Appiah-Menka University of Skills Training and Entrepreneurial Development, Kumasi, Ghana

Student absenteeism in higher education is well documented as a correlate of poor performance, yet it is rarely modeled as a dynamic, socially transmitted process. Existing compartmental treatments either omit the latent phase preceding a first absence or collapse occasional and habitual absence into a single class, and none permits intervention to be targeted by stage. We formulate a five-compartment namely Susceptible–Exposed–Occasional Absentees–Habitual Absentees–Re-engaged (SEACR) model with a graded force of infection, in which exposed, occasional, and habitual students transmit at different weights, and a direct relapse pathway returning re-engaged students to occasional absence without re-exposure. We derive the absenteeism threshold number in closed form and prove that it increases strictly with the relapse rate, that the absenteeism-persistent equilibrium is unique whenever it exists, so that the bifurcation at threshold unity is forward, and that the absenteeism-free equilibrium is globally asymptotically stable. An optimal control problem with three stage-specific controls, namely prevention, early intervention, and remediation, was examined using Pontryagin's maximum principle. For an illustrative cohort, the threshold is 2.4487, and global sensitivity analysis identifies early re-engagement as the most influential recovery parameter, with a partial rank correlation coefficient of −0.894 against −0.825 for remediation. Cost-effectiveness analysis ranks early intervention first under the baseline cost weights, but this ranking changes across alternative assumed cost weights; therefore, single-point cost-effectiveness conclusions should be interpreted cautiously.

KEYWORDS
absenteeism threshold number, compartmental model, cost-effectiveness analysis, Lyapunov stability, Pontryagin's maximum principle, student absenteeism

1 Introduction

Students' absenteeism has become a significant problem in most schools, and particularly at the tertiary level, where attendance behavior does not follow the structured format of pre-tertiary schooling in which teachers monitor absence through a formal register. Chaves-Barboza et al. [1] report that parental financial instability, lack of emotional support, and discomfort in the educational setting all promote absenteeism in mathematics lessons. Using a machine learning approach, Bowen et al. [2] demonstrate that differences in peer interaction separate low-risk from high-risk absenteeism groups, making peer relationships a core underlying factor. Sahin [3] defines absenteeism as a

student's absence from school during the school term without a legitimate reason. Conry and Richards [4] similarly frame it as absence with or without a formal excuse. In this study, we define absenteeism as a deliberate decision by a university student to forgo scheduled academic activities, whether delivered online or face to face, in favor of alternative uses of time. Tola et al. [5] emphasized that academic success in enabling programmes is not determined by a single factor, but rather by a combination of demographic, personal, academic, and institutional variables that interact over time. Concern about absenteeism in tertiary institutions arises not only from its effect on performance but also from its implications for student wellbeing and for the utilization of educational resources. Adu et al. [6] argue that absenteeism impedes the development of accountability and discipline, with consequences for subsequent employment. Goldie [7] notes that high rates of absence depress the morale and performance of educators. In a large-scale meta-analysis of counterproductive academic behaviors, Salgado et al. [8] find absenteeism to be the facet most strongly related to academic performance, reporting a large effect size of $\rho = -0.48$ across 117 independent samples comprising 69,453 students. Delaney and Ashton [9] argue further that class avoidance may signal deteriorating mental health as students struggle with the pressures of university life; hence, absenteeism functions both as an indicator of underlying distress and as a mechanism that intensifies it. Recent evidence also indicates that absenteeism should be understood not only as an individual behavior but as an outcome shaped by academic engagement, institutional practices, and the timing of intervention. A systematic review of factors associated with poor undergraduate academic performance identified low attendance and academic disengagement among the conditions contributing to underperformance [10].

Despite this, most research on university absenteeism remains largely descriptive or correlational. These studies have identified personal, socio-economic, institutional, and peer-level factors that correlate with absenteeism. However, few studies have treated absenteeism as a dynamic, socially transmitted phenomenon. For instance, Adu et al. [6] formulate a four-compartment model of student absenteeism specifically, distinguishing regular attendees, occasional absentees, habitual absentees, and a reintegrated class, and analyse local stability by the Routh–Hurwitz criterion and global stability of the endemic equilibrium by the geometric method of Li and Muldowney [11]. They apply three controls, namely awareness campaigns, class attendance monitoring, and counseling, and conclude that, for cost-effectiveness, class attendance monitoring alone is the most economical strategy.

Compartmental modeling has proved a durable decision-making tool for communicable diseases and for social behaviors transmitted through contact, with recent applications integrating behavioral awareness, threshold analysis, equilibrium stability, and parameter sensitivity into differential-equation frameworks [12–15]. Recent mathematical modeling studies have also extended classical compartmental frameworks through alternative differential-equation formulations and numerical approaches for examining dynamical behavior under different modeling assumptions [16]. Epidemic-style models have been applied to the spread of racism [17] and to smoking behavior [18, 19]. The study by Adu et al. [6] provides important insights into Ghanaian university absenteeism, distinguishing degrees of absence, recognizing that occasional and habitual absence differ in reversibility and in influence, but their model has no latent class: a regular attendee becomes an occasional absentee directly on contact, so the interval during which absenteeism norms are internalized before any class is missed has no representation. Additionally, they permit no relapse other than through renewed exposure and identify the addition of relapse transitions and feedback loops as necessary future work, noting that absenteeism has a cyclical character that a purely linear progression cannot represent. Furthermore, their controls are not stage-specific, so their formulation cannot address what is arguably the central operational question facing a university: whether limited resources are better spent identifying and re-engaging students whose absence is still occasional, or remediating those whose absence has become habitual.

The present study addresses these gaps as we formulate a five-compartment Susceptible-Exposed-Occasional Absentees-Habitual Absentees-Re-engaged (SEACR) model that represents latency and two grades of absence simultaneously, with a graded force of infection in which exposed, occasional, and habitual students transmit absenteeism norms at different relative weights. In addition, we incorporate a direct relapse pathway from the re-engaged class to occasional absence and prove that the absenteeism threshold number is strictly increasing in the relapse rate. Furthermore, we establish that the absenteeism-persistent equilibrium is unique whenever it exists, so that no sub-threshold persistent state coexists with the absenteeism-free equilibrium, and we prove global stability of the absenteeism-free equilibrium by an explicit matrix-theoretic Lyapunov function rather than by inspection. Finally, we formulate an optimal control problem with stage-specific controls, permitting a direct comparison of early intervention against remediation, and we assess the robustness of the resulting cost-effectiveness ranking to the assumed cost weights.

The remainder of the paper is organized as follows. Section 2 presents the model formulation. Section 3 provides the qualitative analysis. Section 4 formulates and characterizes the optimal control problem. Section 5 reports numerical simulations. Section 6 presents the cost-effectiveness analysis and its robustness. Section 7 concludes.

2 Formulating the absenteeism model

2.1 Model structure and assumptions

We consider a cohort of university students of total size $N(t)$, partitioned into five mutually exclusive compartments. The transitions among these compartments are illustrated in Figure 1. The partition is driven by two observations that the existing modeling literature has not combined. First, absenteeism is not adopted instantaneously: students typically pass through a latent phase in which peer rationalization of skipping is internalized before any class is actually missed. Second, absenteeism is not a single state: occasional and habitual absence differs both in how readily they are reversed and in how strongly they influence others. The chain below adapts the latent-class structure of Teklu and Terefe [20], formulated there for animosity

toward mathematics rather than for absenteeism, and extends the graded treatment of absence introduced by Adu et al. [6]. Table 1 presents descriptions of the state variables used in the study.

The parameters used in the study are described in Table 2.

2.2 Force of infection and governing system

Regular attendees acquire absenteeism norms at the rate

$$\lambda(t) = \frac{\beta\left[\theta E(t) + A(t) + \sigma C(t)\right]}{N}. \tag{1}$$

Equation 1 is a standard-incidence form in which all three behaviorally affected classes contribute, weighted by relative influence: θ is below unity because an exposed student expresses the norm verbally but does not yet model it behaviorally, and σ is at or above unity because established absence is the most visible and most readily imitated signal. Setting $\theta = 0$ and $\sigma = 1$ recovers a single-weight model as a special case.

i. Absenteeism norms are transmitted through social contact within the university, at a rate proportional to the weighted prevalence of behaviorally affected students, as in Equation 1.
ii. Adoption is not instantaneous: a student who has internalized the norm passes through a latent phase of mean duration $1/(\kappa+\mu)$ before missing a scheduled activity.
iii. Occasional absence may be reversed directly, without passing through habitual absence, at rate γ_1.
iv. Habitual absence is reached only by escalation from occasional absence, at rate δ.
v. Re-engaged students either recover fully, returning to the regular-attendee compartment at rate ω, or relapse directly into occasional absence at rate φ without requiring further exposure. The second path represents a student whose attendance was restored by intervention but whose underlying disengagement was not resolved.
vi. Exit occurs from every compartment at the common rate μ, balanced by recruitment $\Pi = \mu N$, so that N is constant. This is appropriate for a university observed over 1 or 2 academic years.

$$\begin{aligned}
\frac{dS}{dt} &= \Pi + \omega R - \lambda S - \mu S,\\
\frac{dE}{dt} &= \lambda S - (\kappa+\mu)E,\\
\frac{dA}{dt} &= \kappa E + \phi R - (\delta+\gamma_1+\mu)A,\\
\frac{dC}{dt} &= \delta A - (\gamma_2+\mu)C,\\
\frac{dR}{dt} &= \gamma_1 A + \gamma_2 C - (\omega+\varphi+\mu)R,
\end{aligned} \tag{2}$$

with non-negative initial data. Throughout, the composite parameters are defined in Equation 3 as follows:

$$\begin{aligned}
k_1 = \kappa+\mu, \quad k_2 = \delta+\gamma_1+\mu, \quad k_3 = \gamma_2+\mu, \\
k_4 = \omega+\varphi+\mu.
\end{aligned} \tag{3}$$

2.3 Normalized system

Since N is constant and $\Pi = \mu N$, set $s = \frac{S}{N}$, $e = \frac{E}{N}$, $a = \frac{A}{N}$, $h = \frac{C}{N}$, and $r = \frac{R}{N}$. Dividing Equation 2 by N gives

$$\begin{aligned}
\frac{ds}{dt} &= \mu + \omega r - \beta s\left(\theta e + a + \sigma h\right) - \mu s,\\
\frac{de}{dt} &= \beta s\left(\theta e + a + \sigma h\right) - k_1 e,\\
\frac{da}{dt} &= \kappa e + \phi r - k_2 a,\\
\frac{dh}{dt} &= \delta a - k_3 h,\\
\frac{dr}{dt} &= \gamma_1 a + \gamma_2 h - k_4 r.
\end{aligned} \tag{4}$$

Let $\frac{\Pi}{N} = \mu$. Summing the five equations then gives

$$\frac{d}{dt}\left(s+e+a+h+r\right) = \mu\left[1-\left(s+e+a+h+r\right)\right]$$

Thus, the simplex defined in Equation 5

$$\Omega = \left\{(s,e,a,h,r) \in \mathbb{R}^5_+ : s+e+a+h+r = 1\right\} \tag{5}$$

is invariant and globally attracting.

3 Qualitative analysis

3.1 Positivity and boundedness

Lemma 1. *For non-negative initial data, the solutions of Equation 4 remain non-negative for all $t > 0$, and Ω is positively invariant.*

Proof. On $s = 0$ we have $ds/dt = \mu + \omega r \geq 0$; on $e = 0$, $de/dt = \beta s\left(a+\sigma h\right) \geq 0$; on $a = 0$, $da/dt = \kappa e + \phi r \geq 0$; on $h = 0$, $dc/dt = \delta a \geq 0$; and on $r = 0$, $dr/dt = \gamma_1 a + \gamma_2 h \geq 0$. The vector field is therefore inward-pointing on every boundary face of $\mathbb{R}^5_+$, so no trajectory leaves the positive orthant. Invariance of the simplex follows from the conservation identity in Section 2.3.

3.2 Absenteeism-free equilibrium

Setting the right-hand side of Equation 4 to zero with $e = a = h = r = 0$ gives the unique absenteeism-free equilibrium $\mathcal{E}_0 = (1,0,0,0,0)$.

TABLE 1 Description of state variables.

Compartment	Symbol	Description
Regular attendees	$S(t)$	Students who attend scheduled academic activities regularly and have not internalized absenteeism norms. They are at risk of doing so through social contact.
Exposed	$E(t)$	Students who have internalized absenteeism norms through peer rationalization of skipping, weakened institutional attachment, or diminished motivation but who have not yet missed a scheduled class.
Occasional absentees	$A(t)$	Students who miss scheduled activities intermittently, but not frequently enough for the behavior to be considered established.
Habitual absentees	$C(t)$	Students who miss scheduled activities repeatedly and consistently. Their behavior is established and exerts a stronger influence on peers than that of occasional absentees.
Re-engaged	$R(t)$	Students previously absent who have returned to regular attendance following intervention.

TABLE 2 Description of parameters.

Parameter	Symbol	Meaning
Recruitment rate	Π	Rate at which students enter the university, with $\Pi = \mu N$
Natural exit rate	μ	Exit through graduation, death, transfer, or withdrawal; this rate is equal across compartments
Baseline transmission rate	β	Effective contact rate for transmission of absenteeism norms
Relative influence of exposed students	θ	Influence of an exposed student relative to an occasional absentee, $0 \leq \theta < 1$
Relative influence of habitual absentees	σ	Influence of a habitual absentee relative to an occasional absentee, $\sigma \geq 1$
Progression rate	κ	Rate at which exposed students begin missing classes
Escalation rate	δ	Rate at which occasional absentees become habitual absentees
Early re-engagement rate	γ_1	Rate at which occasional absentees return to regular attendance under routine support
Remediation rate	γ_2	Rate at which habitual absentees are re-engaged through intervention
Full recovery rate	ω	Rate at which re-engaged students return to the regular-attendee compartment
Direct relapse rate	φ	Rate at which re-engaged students revert directly to occasional absence without re-exposure

3.3 The absenteeism threshold number

We compute $\mathcal{R}_0$ by the next-generation matrix method, taking the behaviorally affected compartments in the order $x = (e, a, h, r)^\top$. The class r is retained in this subsystem: because re-engaged students relapse directly into occasional absence at rate φ, the re-engaged class is not absorbing and contributes to onward transmission. This is a structural consequence of assumption (v) with no counterpart in either antecedent model. Since new adoption of absenteeism norms occurs only through entry into the exposed compartment, only the first row of the new-adoption matrix (F) contains non-zero entries; all entries in rows two to four are zero. The new-adoption and transition matrices at $\mathcal{E}_0$ are presented in Equation 6 as follows:

$$\mathcal{F} = \begin{pmatrix} \beta\theta & \beta & \beta\sigma & 0 \\ 0 & 0 & 0 & 0 \\ 0 & 0 & 0 & 0 \\ 0 & 0 & 0 & 0 \end{pmatrix}, \qquad \mathcal{V} = \begin{pmatrix} k_1 & 0 & 0 & 0 \\ -\kappa & k_2 & 0 & -\varphi \\ 0 & -\delta & k_3 & 0 \\ 0 & -\gamma_1 - \gamma_2 & k_4 & \end{pmatrix}. \quad (6)$$

The quantity Δ is defined in Equation 7 as follows:

$$\Delta = k_2 k_3 k_4 - \varphi\left(\gamma_1 k_3 + \gamma_2 \delta\right). \quad (7)$$

Lemma 2. *$\Delta > 0$ for all admissible parameter values.*

Proof. $k_2 k_3 - \left(\gamma_1 k_3 + \gamma_2 \delta\right) = (\delta + \mu)(\gamma_2 + \mu) - \gamma_2 \delta = \mu(\delta + \gamma_2 + \mu) > 0$, so $k_2 k_3 > \gamma_1 k_3 + \gamma_2 \delta$. Since $k_4 = \omega + \varphi + \mu > \varphi$, it follows that $k_2 k_3 k_4 > \left(\gamma_1 k_3 + \gamma_2 \delta\right)\varphi$.

Lemma 2 guarantees $\det \mathcal{V} = k_1 \Delta \neq 0$. Since $\mathcal{F}$ has rank one, the spectral radius of $\mathcal{F}\mathcal{V}^{-1}$ is its $(1,1)$ entry, giving

$$\mathcal{R}_0 = \frac{\beta}{k_1}\left[\theta + \frac{\kappa k_4 \left(k_3 + \sigma\delta\right)}{\Delta}\right]. \quad (8)$$

Expression (Equation 8) admits a direct behavioral reading. The first term is the contribution of the latent phase: a student spends a mean time $1/k_1$ exposed and transmits at the reduced weight θ throughout. The second is the contribution of active absence, weighted by the probability κ/k_1 of progressing from exposure to absence and by the influence accumulated across the occasional and habitual phases. Setting the direct relapse rate $\varphi = 0$ gives the threshold expression presented in Equation 9:

$$\mathcal{R}_0|_{\varphi=0} = \frac{\beta\theta}{k_1} + \frac{\beta\kappa}{k_1 k_2} + \frac{\beta\sigma\kappa\delta}{k_1 k_2 k_3}, \quad (9)$$

the sum of three stagewise contributions, which confirms the derivation.

3.3.1 Comparison with antecedent threshold formulations

To clarify the structural contribution of the present threshold, it is useful to compare it with the two closest antecedent models. Teklu and Terefe [20] consider a susceptible–exposed–animosity–treated system and obtain

$$R_0 = \frac{\beta\gamma}{(\mu+\gamma)(\mu+\delta)}$$

which captures a latent stage followed by a single active behavioral state.

Adu et al. [6], in contrast, distinguish regular attendees, occasional absentees, habitual absentees, and reintegrated students and derive

$$R_0 = \frac{\beta\pi\gamma}{\mu(\mu+\gamma_2)(\delta+\gamma_1+\mu)}$$

The present SEACR threshold extends these formulations by combining a latent stage, separate occasional and habitual absenteeism stages, graded behavioral influence, and a direct relapse pathway from re-engagement to occasional absence. Consequently, the present threshold is not directly reducible to either antecedent expression without imposing additional structural restrictions.

For a numerical comparison, we harmonized the antecedent formulations to the baseline parameter scale of the present model. Because Adu et al. [6] employ count-based mass-action incidence, their transmission coefficient was rescaled to the equivalent standard-incidence form before comparison. Using $\beta = 0.18$, $\mu = 1/48$, $\delta = 0.08$, $\gamma_1 = 0.15$, and $\gamma_2 = 0.05$ gives a harmonized threshold of approximately $R_0 = 0.8105$ for the Adu et al. formulation. For the Teklu and Terefe [20] model, identifying their latent-to-active progression rate with $\kappa = 1/1.5$ and their active-state removal rate with $\gamma_1 = 0.15$ gives $R_0 = 1.0217$. Under the same baseline configuration, the present SEACR model gives $R_0 = 2.4487$. These differences should be interpreted as consequences of model structure rather than as direct empirical differences among student populations.

Proposition 1. *$\mathcal{R}_0$ is strictly increasing in the direct relapse rate φ.*

Proof. Write the bracketed term of Equation 8 as $\theta + \kappa\left(k_3+\sigma\delta\right)/\left[k_2k_3 - \varphi\left(\gamma_1k_3+\gamma_2\delta\right)/k_4\right]$. Since $\varphi/k_4 = \varphi/\left(\omega+\mu+\varphi\right)$ is strictly increasing in φ, the denominator is strictly decreasing in φ and remains positive by Lemma 2.

Proposition 1 has no analog in either antecedent. Re-engagement that is not sustained does not merely fail to help; it raises the threshold, because it returns students to active absence without their having to be re-exposed. Retention of re-engaged students is therefore a control target in its own right.

3.4 Absenteeism-persistent equilibrium

Theorem 1. *System (Equation 4) has no absenteeism-persistent equilibrium when $\mathcal{R}_0 \leq 1$ and exactly one when $\mathcal{R}_0 > 1$, given by*

$$s^* = \frac{1}{\mathcal{R}_0},$$

$$e^* = \frac{1}{\Psi}\left(1-\frac{1}{\mathcal{R}_0}\right)$$

$$a^* = \frac{\kappa k_3k_4}{\Delta}e^*$$

$$h^* = \frac{\kappa\delta k_4}{\Delta}e^*,$$

$$r^* = \frac{\kappa\left(\gamma_1k_3+\gamma_2\delta\right)}{\Delta}e^*, \tag{10}$$

where

$$\psi = 1 + \frac{\kappa\left[k_3k_4+\delta k_4+\gamma_1k_3+\gamma_2\delta\right]}{\Delta}$$

Proof. At equilibrium, the second equation of Equation 4 gives $e^* = \lambda^*s^*/k_1$. The third, fourth, and fifth give $h^* = \delta a^*/k_3$, $r^* = a^*\left(\gamma_1k_3+\gamma_2\delta\right)/\left(k_3k_4\right)$, and $k_2a^* = \kappa e^* + \varphi r^*$. Eliminating r^* gives $a^*\Delta/\left(k_3k_4\right) = \kappa e^*$, hence Equation 10. Substituting into $\lambda^* = \beta\left(\theta e^* + a^* + \sigma h^*\right)$ gives $\lambda^* = k_1\mathcal{R}_0e^*$ by Equation 8; combining with $e^* = \lambda^*s^*/k_1$ yields $\lambda^* = \lambda^*s^*\mathcal{R}_0$, and since $\lambda^* \neq 0$, $s^* = 1/\mathcal{R}_0$. The value of e^* follows from $s^*+e^*+a^*+h^*+r^* = 1$, and $e^* > 0$ if and only if $\mathcal{R}_0 > 1$.

Theorem 1 establishes a forward (transcritical) bifurcation at $\mathcal{R}_0 = 1$. Although relapse mechanisms can generate backward bifurcation in some compartmental models [21], the linear structure of the affected subsystem in the present model excludes such sub-threshold persistence. Thus, within the present model, reducing R_0 below unity is sufficient for elimination of the absenteeism-persistent equilibrium and underpins the threshold-based control analysis in Sections 4–6.

3.5 Local stability

Theorem 2. *$\mathcal{E}_0$ is locally asymptotically stable if $\mathcal{R}_0 < 1$ and unstable if $\mathcal{R}_0 > 1$.*

Proof. Immediate from Theorem 2 of van den Driessche and Watmough [22]: $\mathcal{F} \geq 0$, $\mathcal{V}$ is a non-singular M-matrix by Lemma 2, and the absenteeism-free subsystem $ds/dt = \mu(1-s)$ is globally stable at $s = 1$.

The Jacobian of Equation 4 at a general point is

$$J = \begin{pmatrix} -\lambda-\mu & -\beta\theta s & -\beta s- & \beta\sigma s & \omega \\ \lambda & \beta\theta s & -k_1\beta s & \beta\sigma s & 0 \\ 0 & \kappa & -k_2 & 0 & \varphi \\ 0 & 0 & \delta & -k_3 & 0 \\ 0 & 0 & \gamma_1 & \gamma_2 & -k_4 \end{pmatrix}. \tag{11}$$

Because the characteristic polynomial of Equation 11 at $\mathcal{E}^*$ is quintic with coefficients that do not simplify usefully, we assess local

stability of the persistent equilibrium by direct evaluation of the spectrum of Equation 11 rather than by symbolic Routh–Hurwitz conditions. Section 5.4 reports this verification over the sampled parameter region.

3.6 Global stability of the absenteeism-free equilibrium

The global stability of the absenteeism-free equilibrium is established using the matrix-theoretic Lyapunov construction of Shuai and van den Driessche [23]. The advantage of this approach is that the coefficients of the Lyapunov function are obtained systematically from the next-generation operator rather than selected by inspection.

Let

$$x = (e, a, h, r)^\top$$

denote the vector of behaviorally affected compartments, and write

$$f^\top = \beta(\theta, 1, \sigma, 0),$$

so that the new-adoption matrix can be written in rank-one form as

$$F = e_1 f^\top$$

where $e_1 = (1,0,0,0)^\top$. At the absenteeism-free equilibrium, the next-generation matrix is FV^{-1}, and the absenteeism threshold number is

$$R_0 = \rho(FV^{-1}) = f^\top V^{-1} e_1$$

Define

$$g^\top = f^\top V^{-1}$$

Then

$$\begin{aligned} g^\top F V^{-1} \;\&\; = f^\top V^{-1} e_1 f^\top V^{-1} \\ &= \left(f^\top V^{-1} e_1\right) g^\top \\ &= R_0 g^\top \end{aligned}$$

Thus, $g^\top$ is a positive left Perron eigenvector of the next-generation matrix FV^{-1}.

Theorem 3. If $\mathcal{R}_0 \le 1$, then $\mathcal{E}_0$ is globally asymptotically stable in Ω.

Proof. Define the Lyapunov function in Equation 12 as follows:

$$L = g^\top x = \mathcal{R}_0\, e + g_2\, a + g_3\, h + g_4\, r, \tag{12}$$

where the coefficients are obtained by solving

$$V^\top g = f$$

Solving the coefficient equations gives the expressions presented in Equation 13:

$$\begin{aligned} g_1 &= R_0, \\ g_2 &= \frac{\beta k_4 \left(k_3 + \sigma\delta\right)}{\Delta} \\ g_3 &= \frac{\beta\left[\sigma\Delta + \gamma_2\varphi\left(k_3 + \sigma\delta\right)\right]}{k_3\Delta} \\ g_4 &= \frac{\beta\phi\left(k_3 + \sigma\delta\right)}{\Delta}. \end{aligned} \tag{13}$$

By Lemma 2, all the coefficients are positive. Hence,

$$L(x) \ge 0$$

$\forall\, x \in \Omega$, with $L(x) = 0$ only when

$$e = a = h = r = 0.$$

For the normalized system, the affected subsystem can be written as

$$\dot{x} = sFx - Vx.$$

Since $0 \le s \le 1$ in the invariant region Ω, and $Fx \ge 0$ componentwise,

$$\dot{x} = sFx - Vx \le Fx - Vx = (F - V)x.$$

Differentiating L along the trajectories of the system therefore gives

$$\begin{aligned} \dot{L} &= g^\top \dot{x} \\ &\le g^\top (F - V)\, x \\ &= g^\top F x - g^\top V x. \end{aligned}$$

Because $g^\top = f^\top V^{-1}$,

$$g^\top V = f^\top$$

Moreover,

$$\begin{aligned} g^\top F &= f^\top V^{-1} e_1 f^\top \\ &= R_0 f^\top \end{aligned}$$

Consequently,

$$\dot{L} \le R_0 f^\top x - f^\top x = (R_0 - 1) f^\top x.$$

Since

$$f^\top x = \beta\left(\theta e + a + \sigma h\right) \ge 0,$$

it follows that

$$\dot{L} \le 0 \text{ whenever } R_0 < 1.$$

For $R_0 < 1$, equality $\dot{L} = 0$ requires

$$f^\top x = 0,$$

and, because $\beta, \theta, \sigma > 0$,

$$e = a = h = 0.$$

For a trajectory to remain in this set, the re-engaged compartment must also satisfy $r = 0$. Since the normalized variables sum to unity, this subsequently gives $s = 1$. Therefore, the largest invariant subset of

$$\dot{L} = 0$$

is the absenteeism-free equilibrium

$$E_0 = (1, 0, 0, 0, 0).$$

By LaSalle's [24] invariance principle, E_0 is globally asymptotically stable whenever

$$R_0 < 1.$$

That solving $\mathcal{V}^\top g = f$ independently returns $g_1 = \mathcal{R}_0$ provides a check on expression (Equation 8).

4 Optimal control analysis

4.1 The control problem

We introduce three bounded, Lebesgue-measurable controls on $[0, t_f]$.

- $u_1(t)$ denotes prevention. It comprises institution-wide measures that reduce the effective contact rate through communication of attendance expectations including minimum attendance requirements for examination eligibility, and recognition of students who restore regular attendance. It scales the force of infection to $(1 - u_1)\lambda$.
- $u_2(t)$ denotes early intervention. It comprises attendance monitoring with prompt follow-up. This may include roll call or biometric registration, automatic flagging after a threshold number of absences, and contact by an academic adviser. It augments the early re-engagement rate to $\gamma_1 + \psi_1 u_2$.
- $u_3(t)$ denotes remediation. It comprises counseling, academic support, and structured re-entry for students whose absence is already established. It augments the remediation rate to $\gamma_2 + \psi_2 u_3$.

The constants $\psi_1, \psi_2 > 0$ are the maximum achievable increments in the respective re-engagement rates. The separation of u_2 and u_3 by stage is the purpose of this approach: the controls act on different compartments, so their comparison answers a substantive question about the allocation of institutional resources. The controlled system is

$$\begin{aligned}
\frac{dS}{dt} &= \Pi + \omega R - (1 - u_1)\lambda S - \mu S, \\
\frac{dE}{dt} &= (1 - u_1)\lambda S - k_1 E, \\
\frac{dA}{dt} &= \kappa E + \phi R - (\delta + \gamma_1 + \psi_1 u_2 + \mu) A, \\
\frac{dC}{dt} &= \delta A - (\gamma_2 + \psi_2 u_3 + \mu) C, \\
\frac{dR}{dt} &= (\gamma_1 + \psi_1 u_2) A + (\gamma_2 + \psi_2 u_3) C - k_4 R,
\end{aligned} \tag{14}$$

over the admissible set

$$U = \left\{ (u_1, u_2, u_3) \in \left(L^\infty[0, t_f]\right)^3 : 0 \le u_i(t) \le u_i^{\max} \le 1 \right\}.$$

We minimize

$$J(u_1, u_2, u_3) = \int_0^{t_f} \left[W_1 A + W_2 C + \frac{1}{2}\left(B_1 u_1^2 + B_2 u_2^2 + B_3 u_3^2\right) \right] dt \tag{15}$$

subject to Equation 14, where $W_1, W_2 > 0$ weight the instructional cost of occasional and habitual absence, with $W_2 > W_1$ since established absence carries the larger academic penalty, and $B_1, B_2, B_3 > 0$ are the relative programme costs. The quadratic form reflects increasing marginal cost of intervention intensity.

4.2 Existence

Theorem 4. *There exists an optimal control triple in $\mathcal{U}$ with a corresponding state solution minimizing J.*

Proof. We verify the conditions of Fleming and Rishel [25]. The admissible set is non-empty, since $u_1 = u_2 = u_3 = 0$ is admissible and Equation 14 then reduces to Equation 2, whose solutions exist and are bounded by Lemma 1. $\mathcal{U}$ is closed and convex by construction. The right-hand side of Equation 14 is bounded by a linear function of the state and is Lipschitz in the state uniformly in the controls, since all states are bounded by N and controls by unity. The integrand of Equation 15 is convex in the controls, its Hessian being $diag\ (B_1, B_2, B_3) > 0$. Finally, the integrand is bounded below by $n_1\left(\sum_i |u_i|^2\right)^{n_3/2} - n_2$ with $n_3 = 2$, $n_1 = \frac{1}{2} min\{c_1, c_2, c_3\}$, and $n_2 = 0$, using $W_1 A + W_2 C \ge 0$.

4.3 Characterization

Theorem 5. *Let $\left(u_1^*, u_2^*, u_3^*\right)$ be optimal with associated states. Then there exist adjoint variables $p_1, \ldots, p_5$ satisfying*

$$\begin{aligned}
p_1' &= p_1\left[(1 - u_1)\lambda + \mu\right] - p_2(1 - u_1)\lambda, \\
p_2' &= (p_1 - p_2)\frac{(1 - u_1)\beta\theta S}{N} + k_1 p_2 - \kappa p_3, \\
p_3' &= -W_1 + (p_1 - p_2)\frac{(1 - u_1)\beta S}{N} + p_3(\delta + \gamma_1 + \psi_1 u_2 + \mu) \\
&\quad -\delta p_4 - (\gamma_1 + \psi_1 u_2) p_5, \\
p_4' &= -W_2 + (p_1 - p_2)\frac{(1 - u_1)\beta\sigma S}{N} + p_4(\gamma_2 + \psi_2 u_3 + \mu) \\
&\quad -(\gamma_2 + \psi_2 u_3) p_5, \\
p_5' &= k_4 p_5 - \omega p_1 - \varphi p_3,
\end{aligned} \tag{16}$$

with $p_i\left(t_f\right) = 0$, *and the optimal controls are*

$$u_1^* = min\left\{u_1^{\max}, max\left\{0, \frac{\left(p_2 - p_1\right)\lambda S}{B_1}\right\}\right\},$$
$$u_2^* = min\left\{u_2^{\max}, max\left\{0, \frac{\psi_1 A\left(p_3 - p_5\right)}{B_2}\right\}\right\}, \quad (17)$$
$$u_3^* \& = min\left\{u_3^{\max}, max\left\{0, \frac{\psi_2 C\left(p_4 - p_5\right)}{B_3}\right\}\right\}.$$

Proof. The Hamiltonian associated with the optimal control problem is defined in Equation 18 as follows:

$$\begin{aligned}\mathcal{H} \;=\; & W_1 A + W_2 C + \frac{1}{2}\left(B_1 u_1^2 + B_2 u_2^2 + B_3 u_3^2\right) \\ & + p_1\left[\Pi + \omega R - \left(1 - u_1\right)\lambda S - \mu S\right] + p_2\left[\left(1 - u_1\right)\lambda S - k_1 E\right] \\ & + p_3\left[\kappa E + \phi R - \left(\delta + \gamma_1 + \psi_1 u_2 + \mu\right) A\right] \quad (18) \\ & + p_4\left[\delta A - \left(\gamma_2 + \psi_2 u_3 + \mu\right) C\right] \\ & + p_5\left[\left(\gamma_1 + \psi_1 u_2\right) A + \left(\gamma_2 + \psi_2 u_3\right) C - k_4 R\right].\end{aligned}$$

System (Equation 16) follows from $p_i' = -\partial\mathcal{H}/\partial x_i$, using $\partial\lambda/\partial E = \beta\theta/N$, $\partial\lambda/\partial A = \beta/N$, and $\partial\lambda/\partial C = \beta\sigma/N$. Solving $\partial\mathcal{H}/\partial u_i = 0$ on the interior of $\mathcal{U}$ gives $c_1 u_1 = \left(p_2 - p_1\right)\lambda S$, $c_2 u_2 = \psi_1 A\left(p_3 - p_5\right)$, and $c_3 u_3 = \psi_2 C\left(p_4 - p_5\right)$; projection onto $\left[0, u_i^{\max}\right]$ gives Equation 17.

The characterizations have a clear interpretation. Control u_2 activates precisely when $p_3 > p_5$, that is, when the shadow cost of an additional occasional absentee exceeds that of an additional re-engaged student, and u_3 when $p_4 > p_5$. The relapse rate φ enters p_5' directly, so a cohort with poor retention carries a higher shadow cost on R, which narrows both gaps and depresses both re-engagement controls. This is the dynamic counterpart of Proposition 1.

5 Numerical simulations

5.1 Parameter values

The parameter values in Table 3 are assumed and are chosen to be dimensionally coherent for a university cohort observed over 4 academic years, with time measured in months. The parameter values used in the simulations are therefore illustrative and are not estimates derived from empirical attendance data. Consequently, the numerical results should be interpreted as demonstrations of the behavior of the proposed model rather than as predictions for a specific university cohort. The consequence for interpretation is discussed further in Section 7.

Several parameters have direct structural counterparts in earlier behavioral compartmental models. In particular, β, δ, γ_1, and γ_2 represent transmission, progression from occasional to habitual absenteeism, early re-engagement, and remediation processes that are also represented in the absenteeism model of Adu et al. [6]. The latent-stage progression parameter κ is motivated by the exposed-to-active behavioral transition in Teklu and Terefe [20]. The relative influence parameters θ and σ, together with the direct relapse parameter ϕ, are extensions introduced in the present SEACR formulation to distinguish the behavioral influence of exposed and habitual absentees and to represent relapse after re-engagement. The numerical values assigned to these parameters are illustrative because the antecedent studies do not provide empirically calibrated estimates that can be transferred directly to the present five-compartment model.

TABLE 4 Normalized forward sensitivity indices of $\mathcal{R}_0$.

Parameter	Index	Parameter	Index
β	+1.0000	δ	+0.3050
σ	+0.6231	φ	+0.1624
γ_1	−0.5523	ω	−0.1471
γ_2	−0.4232	θ	+0.0321
μ	−0.3431	κ	−0.0018

The optimality system was solved by the forward–backward sweep method [26] with fourth-order Runge–Kutta integration on a grid of 2,400 intervals over $t_f = 48$ months, controls updated by a weighted convex combination, and convergence declared at a relative tolerance of 10^{-4}; all runs converged within 31 iterations.

With these values, $k_1 = 0.6875$, $k_2 = 0.250833$, $k_3 = 0.070833$, $k_4 = 0.280833$, and $\Delta = 4.11217 \times 10^{-3} > 0$, consistent with Lemma 2. Expression (Equation 8) gives

$$\mathcal{R}_0 = 2.4487.$$

Theorem 1 then gives the absenteeism-persistent equilibrium in proportions $\left(s^*, e^*, a^*, h^*, r^*\right) = (0.4084, 0.0578, 0.1864, 0.2105, 0.1370)$, equivalently $(817, 116, 373, 421, 274)$ students. Substituting these values into the right-hand side of Equation 4 returns residuals of the order of 10^{-18}, and $s^* = 1/\mathcal{R}_0$ holds to machine precision, confirming the algebra of Theorem 1.

5.2 Model dynamics

Figure 2 shows the uncontrolled trajectories under two transmission regimes. At $\beta = 0.18$, giving $\mathcal{R}_0 = 2.4487$, the regular-attendee class declines from 1,700 to approximately 880 over 4 years while occasional and habitual absence rise toward the predicted equilibrium, confirming Theorem 2. At $\beta = 0.06$, giving $\mathcal{R}_0 = 0.8162$, all four affected classes decay toward zero and the cohort returns to full regular attendance, consistent with Theorem 3.

5.3 Sensitivity analysis

Normalized forward sensitivity indices computed from Equation 8 are given in Table 4. As theory requires, $\chi_\beta^{\mathcal{R}_0} = 1$ exactly, since $\mathcal{R}_0$ is linear in β; this serves as a check on the numerical differentiation.

TABLE 3 Assumed parameter values.

Parameter	Value	Unit	Basis
N	2,000 students	students	Illustrative faculty-sized cohort
μ	1/48	month^{-1}	Mean 4-year residence
β	0.18	month^{-1}	Assumed
θ	0.30	dimensionless	Assumed; exposed students transmit at reduced weight
σ	1.60	dimensionless	Assumed; habitual absence is more visible
κ	1/1.5	month^{-1}	Mean latency 1.5 months
δ	0.08	month^{-1}	Assumed
γ_1	0.15	month^{-1}	Assumed
γ_2	0.05	month^{-1}	Assumed; habitual absence is harder to reverse
ω	0.20	month^{-1}	Assumed
φ	0.06	month^{-1}	Assumed
ψ_1, ψ_2	0.50, 0.40	month^{-1}	Maximum control-induced increments
W_1, W_2	1, 3	dimensionless	Relative burden of occasional and habitual absence
B_1, B_2, B_3	50, 30, 80	model cost units	Relative programme costs
$u_i^{\max}$	0.9	dimensionless	Maximum feasible intervention intensity

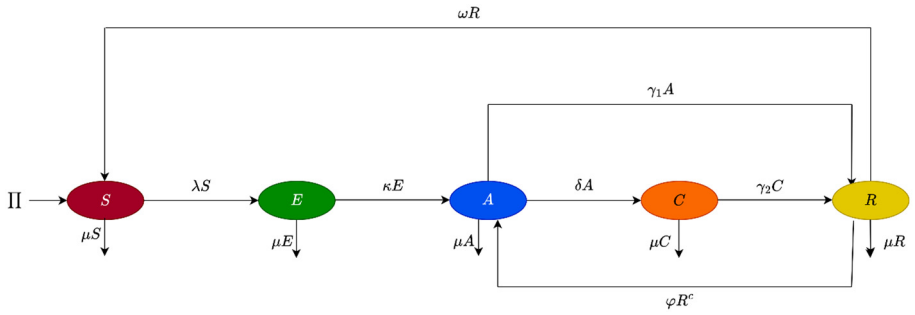


FIGURE 1
Schematic diagram of the Susceptible–Exposed–Occasional Absentees–Habitual Absentees–Re-engaged (SEACR) absenteeism model. Red represents susceptible students (S), green represents exposed students (E), blue represents occasional absentees (A), orange represents habitual absentees (C), and yellow represents re-engaged students (R). Early re-engagement γ1A carries occasional absentees directly to the re-engaged class without passing through habitual absence, while φR returns re-engaged students to occasional absence without re-exposure.

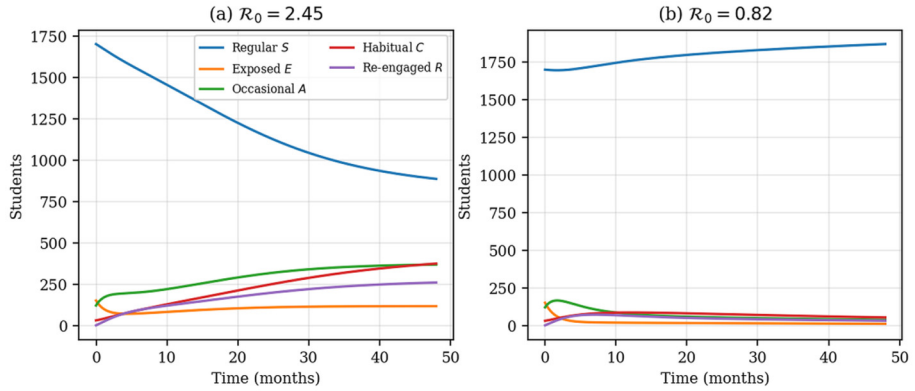


FIGURE 2
Uncontrolled dynamics of the SEACR model. **(a)** $\mathcal{R}_0 = 2.45$; **(b)** $\mathcal{R}_0 = 0.82$. Note that habitual absence overtakes the re-engaged class within the first year and continues to accumulate. The habitual compartment is the slowest to fill and the slowest to empty, since $k_3 = 0.0708$ is the smallest of the four composite rates: once absence becomes established, it is highly persistent, which is precisely the argument for intervening before it does.

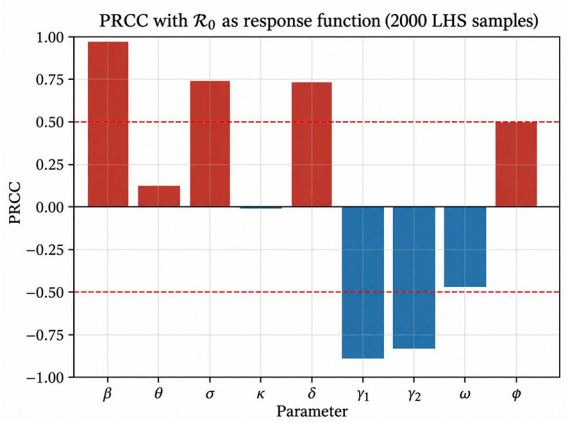


FIGURE 3
Partial rank correlation coefficients (PRCCs) of the model parameters with R_0 as the response function, based on 2,000 Latin hypercube samples. The dashed lines at PRCC = +0.5 and PRCC = −0.5 are visual guides for comparatively strong positive and negative associations, respectively. LHS, Latin hypercube sampling.

TABLE 5 Partial rank correlation coefficients (PRCCs; $\mathcal{R}_0$ as the response, $n = 2,000$).

Parameter	PRCC	*p-value*
β	+0.9678	$< 10^{-15}$
σ	+0.7387	$< 10^{-15}$
δ	+0.7254	$< 10^{-15}$
φ	+0.4940	$< 10^{-15}$
θ	+0.1235	3.2×10^{-8}
κ	−0.0023	0.918
ω	−0.4665	$< 10^{-15}$
γ_2	−0.8253	$< 10^{-15}$
γ_1	−0.8944	$< 10^{-15}$

Global sensitivity analysis was performed by Latin hypercube sampling of 2,000 parameter sets over ±50% of the baseline values, with $\mathcal{R}_0$ as the response function; partial rank correlation coefficients (PRCCs) are shown in Figure 3 and Table 5.

The dashed horizontal lines at PRCC ±0.5 are included only as visual reference points for identifying parameters with comparatively strong positive or negative monotonic relationships with R_0; they are not statistical significance thresholds.

The results first show that the early re-engagement rate γ_1 is the most influential protective parameter, with $|-0.8944|$ exceeding the value $|-0.8253|$ of the remediation rate γ_2, and the same ordering appears in the local indices (−0.5523 against −0.4232). A given proportional improvement in the rate at which occasional absentees are recovered reduces the threshold more than the same proportional improvement in the rate at which habitual absentees are remediated. This is a structural result about where in the progression intervention has the most leverage, and it does not depend on any cost assumption. Second, the relapse rate (ϕ) has a substantial positive PRCC of +0.4940, confirming Proposition 1 numerically across the sampled region and establishing relapse as an important driver of absenteeism persistence. The escalation rate (δ) also has a positive association with the absenteeism threshold, indicating that faster progression from occasional to habitual absence contributes to absenteeism persistence.

The positive association between relapse and the threshold indicates that the benefits of re-engagement are less durable when students return rapidly to occasional absenteeism. Third, κ is not significantly associated with $\mathcal{R}_0$ ($PRCC = -0.0023$, $p = 0.918$), matching its near-zero local index. This is initially surprising but follows from Equation 8 as lengthening the latent phase delays progression to absence without preventing it, and the two effects—longer time transmitting at weight θ and later arrival in the higher-weight classes—very nearly cancel. Within the assumed parameter configuration, slowing progression from exposure to absence has relatively limited influence on the threshold unless progression is also interrupted through re-engagement or related support.

Figure 4 presents contour plots of $\mathcal{R}_0$ over (γ_1, γ_2) and over (β, φ), with the critical contour $\mathcal{R}_0 = 1$ marked. Figure 4a shows that the critical contour is reached at more modest values of γ_1 than of γ_2; Figure 4b shows that the transmission rate required for persistence falls as relapse rises.

5.4 Local stability of the persistent equilibrium

At the baseline parameter values, the Jacobian (Equation 11) evaluated at $\mathcal{E}^*$ has the spectrum

$$\{-0.766459,\ -0.266006 \pm 0.096369i,\ -0.066756,\ -0.020833\},$$

all of which have negative real parts, so $\mathcal{E}^*$ is locally asymptotically stable. The complex pair indicates a damped oscillatory approach, consistent with the shoulder visible in the occasional-absentee trajectory of Figure 2a.

To establish that this is not an artifact of the particular parameter choice, we drew 5,000 parameter sets from the same Latin hypercube region used in Section 5.3, retained the 4,935 for which $\mathcal{R}_0 > 1$, and computed the spectrum of Equation 11 at the corresponding persistent equilibrium in each case. In every one of the 4,935 cases, the maximum real part was strictly negative, the largest value observed across the whole sample being -2.396×10^{-4}. Across the sampled parameter region, all 4,935 parameter sets for which the absenteeism-persistent equilibrium exists produced Jacobian eigenvalues with strictly negative maximum real parts. Thus, the persistent equilibrium is locally asymptotically stable for every parameter configuration examined. This finding provides strong numerical evidence that local stability is robust within the investigated parameter region. It should not, however, be interpreted as a proof of global asymptotic stability. Numerical verification, regardless of the number of parameter sets examined, cannot exclude qualitatively different behavior outside the sampled region or establish convergence of every admissible trajectory to the persistent equilibrium.

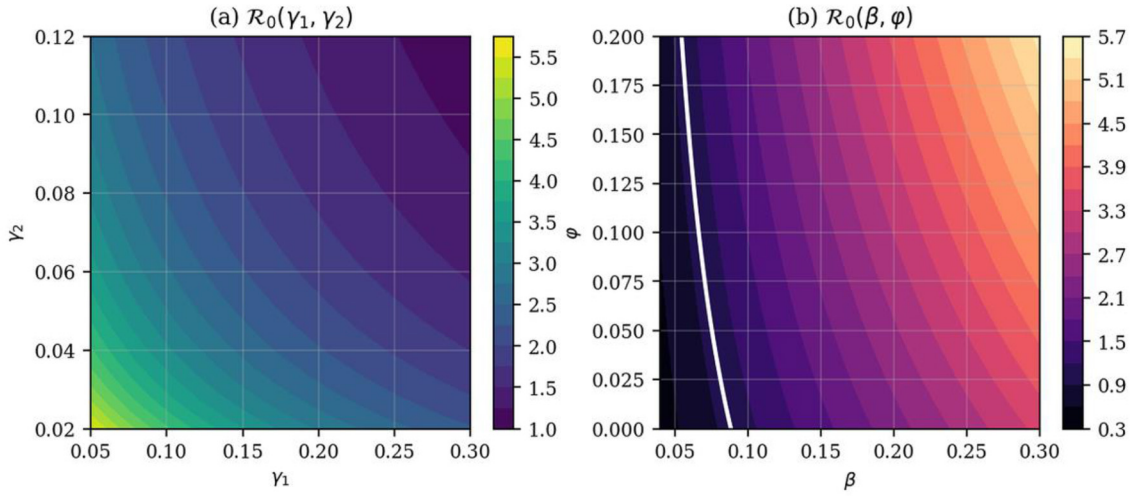


FIGURE 4
Contour plots of the absenteeism threshold number. The white contour marks $\mathcal{R}_0 = 1$. **(a)** $\mathcal{R}_0 = (\gamma_1, \gamma_2)$; **(b)** $\mathcal{R}_0 = (\beta, \varphi)$.

5.5 Optimal control simulations

Seven strategies were simulated: each control singly, each pair, and all three. Figure 5 shows the occasional and habitual absentee trajectories under each, against the uncontrolled baseline. Figure 6 shows control profiles for Strategies 2, 3, and 7.

The single-control profiles remain close to the upper bound of 0.9 for about 45 months before declining near the end of the intervention period. This pattern reflects the way the assumed absenteeism-burden weights, intervention costs, and terminal conditions interact in the model. It should not be interpreted as a recommendation for universities to maintain maximum intervention intensity continuously for almost 4 academic years. Rather, under the present model assumptions, sustained intervention continues to produce greater benefits than costs for most of the simulation period.

In practice, maintaining such a high level of intervention for this length of time may be difficult. Universities operate under staffing, counseling, monitoring, budgetary, and other implementation constraints that are not explicitly represented in the model. Future extensions could therefore incorporate cumulative budget limits, capacity constraints, time-varying intervention costs, or alternative cost structures to produce control profiles that more closely reflect real institutional conditions. The control trajectories reported here should thus be understood as mathematical optima under the assumed model structure and cost weights, rather than as exact operational schedules.

Under Strategy 7, the control profiles begin to taper from about month 10, and each intervention is applied at a lower intensity than when used alone. This is because the three controls act at different stages of the absenteeism process and partly complement or substitute for one another. Notably, u_2 remains the most intensively applied control during the tapering phase, which is consistent with the sensitivity analysis. Over the 48-month simulation period, the uncontrolled cohort accumulates 25,095.5 student-months of absence. Under the assumed parameter values, Strategy 7 averts 24,278.0 student-months, representing 96.7% of the uncontrolled burden and the largest reduction among the seven strategies considered. By comparison, Strategy 3, which relies on remediation alone, averts 15,610.8 student-months of absence and is the least effective of the single-control strategies because it intervenes only after absenteeism has become established.

6 Cost-effectiveness analysis

6.1 ACER and ICER

The average cost-effectiveness ratio (ACER) measures the average intervention cost required to avert one unit of absenteeism and is calculated as the total intervention cost divided by the total absenteeism averted. The incremental cost-effectiveness ratio (ICER) compares two strategies and represents the additional cost required to obtain one additional unit of absenteeism averted when moving from a less effective strategy to a more effective strategy. Accordingly, the average cost-effectiveness ratio (ACER) and incremental cost-effectiveness ratio (ICER) are computed using Equation 19 as follows:

$$\text{ACER} = \frac{\text{total intervention cost}}{\text{absenteeism averted}}, \quad \text{ICER}_{i,j} = \frac{\text{cost}_i - \text{cost}_j}{\text{averted}_i - \text{averted}_j}, \quad (19)$$

Thus, ACER represents the average model-based intervention cost per student-month of absenteeism averted, whereas ICER represents the additional cost per additional student-month of absenteeism averted when one strategy is compared with another.

With total cost $CT = \frac{1}{2}\int_0^{tf}\left(B_1u_1^2 + B_2u_2^2 + B_3u_3^2\right)dt$, absenteeism averted is measured as $\int_0^{tf}\left[(A+C)_{no\ control} - (A+C)_{control}\right]dt$, in student-months of absence rather than in headcount. This distinction is stated explicitly because the antecedent literature is not consistent on the measure used.

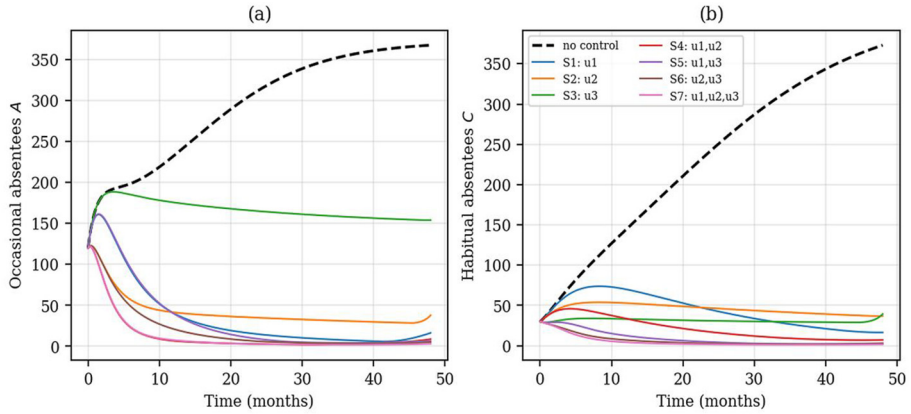


FIGURE 5
(a) Occasional and **(b)** Habitual absentee trajectories under all seven control strategies, against the uncontrolled baseline (dashed).

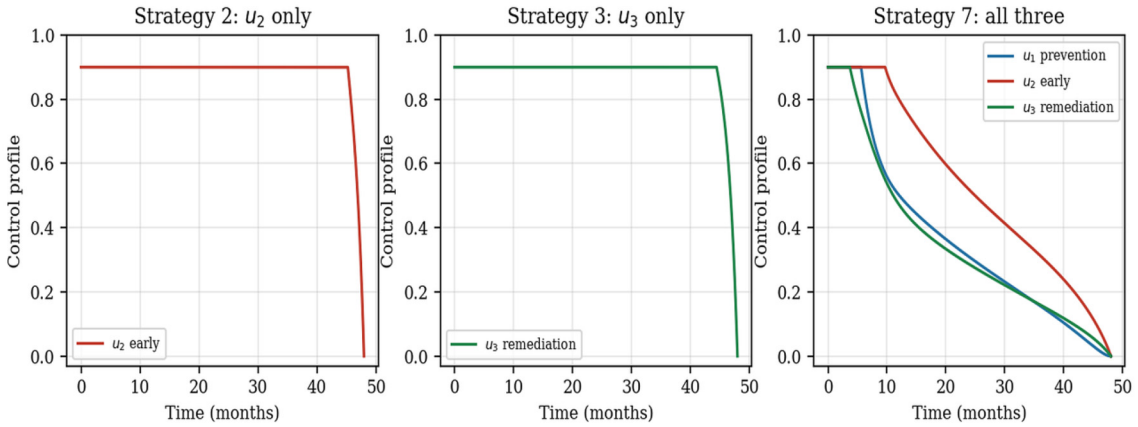


FIGURE 6
Optimal control profiles for Strategies 2, 3, and 7.

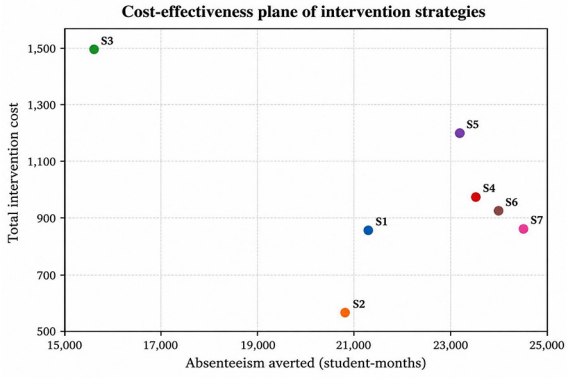


FIGURE 7
Cost-effectiveness plane showing total intervention cost against absenteeism averted for Strategies S1–S7.

Strategy 2 has the lowest ACER at 0.027021 and Strategy 3 the highest at 0.095938, a factor of 3.6. The relationship between total intervention cost and absenteeism averted across the seven intervention strategies is illustrated in Figure 7. Strategy 7 costs less than Strategies 4, 5, and 6 while averting more, because the three controls substitute for one another and each is used less intensively, as Figure 6 shows; combined strategies are not simply the sum of their parts. Additionally, under these weights, remediation alone is both the most expensive and the least effective single strategy. Its low effectiveness is a property of the model structure and does not depend on the costing; its high cost does, as Section 6.2 shows.

Recursive ICER elimination proceeds as follows. Strategy 1 is eliminated first, having the highest incremental ratio at 0.7299; then Strategy 5 at 0.2882, Strategy 4 at 0.1553, Strategy 6 at 0.1210, and Strategy 3 at 0.0959. The final comparison is between Strategies 2 and 7, with $ICER = 0.0892$ for Strategy 7 against an ACER of 0.0270 for Strategy 2. Strategy 2, representing early intervention among occasional absentees, survives the recursive elimination procedure.

6.2 Robustness of the ranking

The conclusion of Section 6.1 rests on the assumed cost weights $(B_1, B_2, B_3) = (50,\ 30,\ 80)$, and its sensitivity to alternative

assumptions should be assessed. We therefore recomputed the full seven-strategy comparison across a grid of cost weights. Table 6 reports the ACER-minimizing strategy at selected points of the grid $B_2, B_3 \in [15,\ 110]$ with B_1 fixed at 50.

The ranking is not robust. Hence, early intervention is preferred when it is inexpensive relative to remediation. The combined strategy becomes preferred once the two are comparably priced. Prevention alone is preferred when it is inexpensive relative to both; most strikingly, when remediation is made inexpensive ($B_3 = 15$), the ACER criterion selects Strategy 3 (remediation alone) despite its averting the least absence of any strategy in Table 7. That last case exposes a limitation of ACER itself as a selection criterion (a strategy can minimize cost per unit averted while leaving most of the burden in place). Since none of B_1, B_2, or B_3 is estimated from data here or in the antecedent literature, the ordering of strategies by ACER should be regarded as conditional on an unverified assumption. This matters beyond the present paper. Adu et al. [6] conclude that class attendance monitoring alone is the most cost-effective strategy for reducing absenteeism, on the basis of a single set of assumed weights and without a robustness check. Our Strategy 2 is the closest analog of their recommended strategy, and we reach the same conclusion under the baseline cost weights. However, the preferred strategy changes under alternative assumed cost configurations. We therefore regard the more general qualitative result as the defensible one: early intervention tends to outperform late remediation under the baseline behavioral parameterization, a finding that is also supported by the PRCC ordering independently of the assumed cost weights. The finer ranking among the remaining strategies should be interpreted as conditional on the assumed programme-cost structure.

6.3 Robustness to model-parameter variation

To complement the cost-weight analysis, we examined whether the optimal-control profiles and cost-effectiveness ranking were sensitive to uncertainty in key behavioral parameters. The transmission rate β, early re-engagement rate γ_1, remediation rate γ_2, relapse rate φ, and escalation rate δ were each varied independently by $\pm 20\%$ around their baseline values, while all other parameters and cost weights were held fixed. For each scenario, the optimality system was re-solved for all seven strategies and the corresponding absenteeism averted, intervention cost, ACER, and control trajectories were recalculated. The results of the parameter perturbation analysis are summarized in Table 8. Across all 10 perturbation scenarios, Strategy 2 retained the lowest ACER, while Strategy 7 retained the second-lowest ACER. Thus, the leading cost-effectiveness ordering was stable under the moderate one-at-a-time parameter variations considered here. The optimal-control intensities, however, changed quantitatively across scenarios. For Strategy 7, the time-averaged value of u_1 ranged from 0.302 to 0.416, u_2 from 0.509 to 0.556, and u_3 from 0.333 to 0.367 over the 48-month intervention horizon. Higher transmission increased the required prevention intensity, lower baseline early re-engagement increased the optimal intensity of u_2, and higher relapse increased the overall intensity of the combined intervention. These results suggest that, within the $\pm 20\%$ perturbation range examined, uncertainty in behavioral parameters affects the magnitude of the optimal intervention effort more strongly than the leading cost-effectiveness ranking.

7 Discussion and conclusion

We have formulated and analyzed a five-compartment model of university student absenteeism that represents latency and two grades of absence simultaneously, with a graded force of infection and a direct relapse pathway. The closed-form threshold number (Equation 8) reduces to neither of the expressions obtained by Adu et al. [6] or Teklu and Terefe [20], and decomposes interpretably into stagewise contributions. We proved that its denominator is positive for all admissible parameters (Lemma 2), that it increases strictly with relapse (Proposition 1), and that the persistent equilibrium is unique whenever it exists, so the bifurcation is forward (Theorem 1). Global stability of the absenteeism-free equilibrium was established by an explicit Lyapunov function derived from the left Perron eigenvector rather than constructed by inspection (Theorem 3).

Three substantive findings emerge. First, within the assumed parameter configuration, the model identifies the transition out of occasional absence as the point of greatest leverage: the early re-engagement rate carries the largest protective PRCC and local sensitivity index, while remediation alone is the weakest single-control strategy in the simulations. This result should be interpreted as a structural and model-based finding rather than as an empirically established ranking of real university interventions. Second, higher relapse after re-engagement increases the absenteeism threshold, indicating that the benefits of re-engagement are less durable when students return quickly to occasional absence. This result should be understood as a consequence of the modeled relapse pathway rather than as evidence that re-engagement interventions are themselves harmful. Third, under the assumed parameter configuration, the duration of the latent phase has comparatively little influence on the threshold, whereas interruption of progression from exposure to active absenteeism exerts a substantially stronger effect.

The intervention comparisons should also be interpreted within the scope of the outcomes represented in the model. The present framework evaluates intervention benefits mainly through reductions in absenteeism and transitions between attendance states. It does not capture other potential benefits of attendance monitoring, counseling, preventive communication, or academic support, such as improved motivation, student engagement, retention, wellbeing, or access to support services. Consequently, a strategy that appears less effective in reducing absenteeism within the model may still provide important educational or psychosocial benefits that are not represented by the present state variables.

7.1 Limitations

The most serious limitation is that no empirical attendance data were used: all parameters in Table 3 are assumed, and the numerical results are therefore illustrative of the model's behavior rather than estimates for any real cohorts. A further theoretical limitation

TABLE 6 ACER-minimizing strategy at selected cost weights.

c_1	c_2	c_3	Best strategy	ACER
50	30	80	2 (u_2)	0.027021
50	15	100	2 (u_2)	0.013743
50	30	30	2 (u_2)	0.027021
50	80	30	7 (all three)	0.036176
50	50	50	7 (all three)	0.035859
50	60	40	7 (all three)	0.035676
20	60	60	1 (u_1)	0.016992
50	30	15	3 (u_3)	0.01794
50	70	15	3 (u_3)	0.01794

TABLE 7 Absenteeism averted, cost, and average cost-effectiveness ratio (ACER) by strategy (ascending in absenteeism averted).

Strategy	Controls	Averted (student-months)	Cost	ACER
3	u_3	15,610.84	1,497.67	0.095938
2	u_2	20,898.22	564.69	**0.027021**
1	u_1	21,302.77	859.97	0.040369
5	u_1, u_3	23,106.18	1,201.03	0.051979
4	u_1, u_2	23,459.12	962.35	0.041023
6	u_2, u_3	23,849.50	921.86	0.038653
7	u_1, u_2, u_3	24,278.03	866.32	0.035683

Bold values indicate the highlighted results for the corresponding cost-effectiveness measures.

TABLE 8 Robustness of cost-effectiveness ranking and Strategy 7 control intensity to ±20% parameter perturbations.

Scenario	Lowest-ACER strategy	Lowest ACER	Mean u_1, Strategy 7	Mean u_2, Strategy 7	Mean u_3, Strategy 7
Baseline	2	0.0270	0.366	0.533	0.352
$\beta - 20\%$	2	0.0343	0.302	0.509	0.344
$\beta + 20\%$	2	0.0233	0.416	0.535	0.349
$\gamma_1 - 20\%$	2	0.0230	0.381	0.556	0.356
$\gamma_1 + 20\%$	2	0.0317	0.352	0.512	0.347
$\gamma_2 - 20\%$	2	0.0260	0.371	0.536	0.364
$\gamma_2 + 20\%$	2	0.0280	0.362	0.531	0.340
$\varphi - 20\%$	2	0.0276	0.348	0.516	0.345
$\varphi + 20\%$	2	0.0265	0.384	0.548	0.358
$\delta - 20\%$	2	0.0281	0.347	0.531	0.333
$\delta + 20\%$	2	0.0262	0.383	0.534	0.367

ACER, average cost-effectiveness ratio.

is that global asymptotic stability of the absenteeism-persistent equilibrium has not been established analytically. Although local stability was verified numerically for all 4,935 sampled parameter configurations satisfying the persistence condition, this constitutes numerical evidence rather than a global stability theorem. Consequently, the analysis does not establish that every admissible solution converges to the persistent equilibrium whenever the absenteeism threshold exceeds unity. Establishing such a result through an appropriate Lyapunov, graph-theoretic, or geometric method remains an important theoretical extension of the present model. The assumption of a constant cohort size is reasonable over 1 or 2 academic years but would need relaxing over longer horizons, as would the assumption of homogeneous mixing, which ignores programme, year-group, and residential structure. Transmission is taken to be time-invariant, whereas university attendance is strongly periodic across a semester; a time-dependent $\beta(t)$ with a semester period would be a natural and, to our knowledge, unexplored extension. Finally, the cost weights are assumed rather than costed, which is why Section 6.2 is included and why we decline to rest any conclusion on the finer ACER

ranking. The model also does not capture the full range of benefits that may arise from the interventions considered, since its evaluation is restricted mainly to absenteeism-related transitions and accumulated absence. Broader outcomes, including academic performance, engagement, retention, motivation, and wellbeing, remain outside the present framework.

7.2 Future work

Fitting β, κ, δ, and γ_1 to attendance registers from a Ghanaian university, with confidence intervals propagated through to the cost-effectiveness ratios, would convert the present illustrative results into estimates. Such empirical calibration would parallel recent developments in dynamical modeling in which model parameters and trajectories are evaluated against observed population data instead of being based exclusively on assumed parameter values [27, 28]. Beyond this, a saturated incidence of the form $\beta(\theta E + A + \sigma C) / (1 + \alpha(A + C))$ would relax the assumption that influence scales linearly with prevalence and could admit backward bifurcation, which the present formulation excludes; and a fourth control acting directly on φ would allow retention to be costed against the other three. The present model therefore provides theoretical support for the hypothesis that detecting and responding to absenteeism while it remains occasional may offer greater leverage than intervention initiated only after absenteeism becomes habitual. It also indicates that the effectiveness of re-engagement depends partly on limiting subsequent relapse. Because the model has not yet been calibrated to empirical attendance data, these findings should be interpreted as theoretically derived and numerically illustrated propositions that require validation using longitudinal university attendance records. An important theoretical direction is to establish conditions for global asymptotic stability of the absenteeism-persistent equilibrium when the threshold exceeds unity. The numerical evidence reported in Section 5.4 suggests a stable persistent state throughout the parameter region examined, but an analytical result is still required. Future work may investigate whether the graph-theoretic Lyapunov framework of Shuai and van den Driessche [23], the geometric approach associated with Li–Muldowney-type methods, or another suitable Lyapunov construction can establish global convergence for the present five-dimensional system.

Data availability statement

The original contributions presented in the study are included in the article/supplementary material, further inquiries can be directed to the corresponding author.

Author contributions

FB: Formal analysis, Methodology, Writing – review & editing, Software, Validation, Visualization. EL: Conceptualization, Formal analysis, Methodology, Writing – review & editing, Writing – original draft.

Funding

The author(s) declared that financial support was not received for this work and/or its publication.

Conflict of interest

The author(s) declared that this work was conducted in the absence of any commercial or financial relationships that could be construed as a potential conflict of interest.

Generative AI statement

The author(s) declared that Generative AI was not used in the creation of this manuscript.

Any alternative text (alt text) provided alongside figures in this article has been generated by Frontiers with the support of artificial intelligence and reasonable efforts have been made to ensure accuracy, including review by the authors wherever possible. If you identify any issues, please contact us.

Publisher's note

All claims expressed in this article are solely those of the authors and do not necessarily represent those of their affiliated organizations, or those of the publisher, the editors and the reviewers. Any product that may be evaluated in this article, or claim that may be made by its manufacturer, is not guaranteed or endorsed by the publisher.

References

1. Chaves-Barboza E, Marín-Marín JA, Sarmento-Dos-Santos AP, Trujillo-Torres JM. Student absenteeism in mathematics lessons: Social variables in the PGS of Namibe. *Educ Sci.* (2019) 9:130. doi: 10.3390/educsci9020130

2. Bowen F, Gentle-Genitty C, Siegler J, Jackson M. Revealing underlying factors of absenteeism: a machine learning approach. *Front Psychol.* (2022) 13:958748. doi: 10.3389/fpsyg.2022.958748

3. Sahin M. A study on absenteeism of university students. *Int e-J Educ Stud.* (2023) 7:75–88. doi: 10.31458/iejes.1223043

4. Conry JM, Richards MP. The severity of state truancy policies and chronic absenteeism. *J Educ Stud Placed Risk*. (2018) 23:187–203. doi: 10.1080/10824669.2018.1439752

5. Tola M, Belay DB, Zeru MA, Adegeh SC. Joint modeling of exam results and attrition status of students at Hawassa College of Education, Ethiopia. *Educ Res Int.* (2022) 2022:8919604. doi: 10.1155/2022/8919604

6. Adu IK, Asamoah JKK, Wireko FA, Afosaa V, Foriwaa KA. Mathematical modelling of absenteeism with optimal control analysis. *Qual Quant.* (2026) 60:6899–938. doi: 10.1007/s11135-025-02566-0

7. Goldie J. Classroom attendance in higher education: a systematic literature review. In: *ICERI2009 Proceedings.* (2009). p. 2540–9.

8. Salgado JF, Cuadrado D, Moscoso S. Counterproductive academic behaviors and academic performance: a meta-analysis and a path analysis model. *Front Psychol.* (2022) 13:893775. doi: 10.3389/fpsyg.2022.893775

9. Delaney E, Ashton M. Does an attendance policy positively impact staff and student wellbeing? A case study exploring attitudes toward a University of Surrey attendance policy. *J Hosp Tour Educ.* (2024) 36:205–15. doi: 10.1080/10963758.2024.2369131

10. Al-Tameemi RAN, Johnson C, Gitay R, Abdel-Salam ASG, Al Hazaa K, BenSaid A, et al. Determinants of poor academic performance among undergraduate students—A systematic literature review. *Int J Educ Res Open.* (2023) 4:100232. doi: 10.1016/j.ijedro.2023.100232

11. Li MY, Muldowney JS. A geometric approach to global-stability problems. *SIAM J Math Anal.* (1996) 27:1070–83. doi: 10.1137/S0036141094266449

12. Hussain S, Zeb A, Rasheed A, Saeed T. Stochastic mathematical model for the spread and control of coronavirus. *Adv Differ Equ.* (2020) 2020:574. doi: 10.1186/s13662-020-03029-6

13. Jiru MT, Kumaravel SK. Stability and sensitivity analysis of a pneumonia model with awareness component using differential equations. *Fix Point Theory Algor Sci Eng.* (2026) 2026:5. doi: 10.1186/s13663-025-00815-3

14. Masood Z, Samar R, Raja MAZ. Design of fractional order epidemic model for future generation tiny hardware implants. *Future Gener Comput Syst.* (2020) 106:43–54. doi: 10.1016/j.future.2019.12.053

15. Teklu SW, Rao KP. HIV/AIDS-pneumonia codynamics model analysis with vaccination and treatment. *Comput Math Methods Med.* (2022) 2022:3105734. doi: 10.1155/2022/3105734

16. Jiru MT, Mekonen KG. Modeling enteric fever transmission dynamics: a comparative analysis of local and nonlocal boundary value approaches. *Bound Value Probl.* (2025) 2025:33. doi: 10.1186/s13661-024-01988-3

17. Mamo DK. Modeling the spread dynamics of racism in cyberspace. *J Math Model.* (2020) 8:105–22. doi: 10.22124/jmm.2020.14850.1346

18. Khyar O, Danane J, Allali K. Mathematical analysis and optimal control of giving up the smoking model. *Int J Differ Equ.* (2021) 2021:8673020. doi: 10.1155/2021/8673020

19. Sofia IR, Bandekar SR, Ghosh M. Mathematical modeling of smoking dynamics in society with impact of media information and awareness. *Results Control Optim.* (2023) 11:100233. doi: 10.1016/j.rico.2023.100233

20. Teklu SW, Terefe BB. Mathematical modeling analysis on the dynamics of university students animosity towards mathematics with optimal control theory. *Sci Rep.* (2022) 12:11578. doi: 10.1038/s41598-022-15376-3

21. Castillo-Chavez C, Song B. Dynamical models of tuberculosis and their applications. *Math Biosci Eng.* (2004) 1:361–404. doi: 10.3934/mbe.2004.1.361

22. van den Driessche P, Watmough J. Reproduction numbers and sub-threshold endemic equilibria for compartmental models of disease transmission. *Math Biosci.* (2002) 180:29–48. doi: 10.1016/S0025-5564(02)00108-6

23. Shuai Z, van den Driessche P. Global stability of infectious disease models using Lyapunov functions. *SIAM J Appl Math.* (2013) 73:1513–32. doi: 10.1137/120876642

24. LaSalle JP. *The Stability of Dynamical Systems*. Philadelphia, PA: Society for Industrial and Applied Mathematics. (1976).

25. Fleming WH, Rishel RW. *Deterministic and Stochastic Optimal Control*. New York, NY: Springer (1975).

26. Lenhart S, Workman JT. *Optimal Control Applied to Biological Models*. Boca Raton, FL: Chapman and Hall/CRC (2007).

27. Jiru MT, Kumaravel SK. A memory-driven pneumonia dynamics model validated against Ethiopian mortality data: a fractional-order differential equation framework. *Sci Rep.* (2026) 16:21201. doi: 10.1038/s41598-026-56464-y

28. Jiru MT, Kumaravel SK. Memory effects in tuberculosis–pneumonia co-dynamics: a Caputo fractional-order difierential equation framework validated against Ethiopian data. *Discover Appl Sci.* (2026) s42452-026-09294-6. doi: 10.1007/s42452-026-09294-6